



# CANCER DISCOVERY

## A Diverse Array of Cancer-Associated *MTOR* Mutations Are Hyperactivating and Can Predict Rapamycin Sensitivity

Brian C. Grabiner, Valentina Nardi, Kivanç Birsoy, et al.

*Cancer Discovery* 2014;4:554-563. Published OnlineFirst March 14, 2014.

**Updated version** Access the most recent version of this article at:  
doi:[10.1158/2159-8290.CD-13-0929](https://doi.org/10.1158/2159-8290.CD-13-0929)

**Supplementary Material** Access the most recent supplemental material at:  
<http://cancerdiscovery.aacrjournals.org/content/suppl/2014/03/13/2159-8290.CD-13-0929.DC1.html>

**Cited Articles** This article cites by 40 articles, 14 of which you can access for free at:  
<http://cancerdiscovery.aacrjournals.org/content/4/5/554.full.html#ref-list-1>

**Citing articles** This article has been cited by 1 HighWire-hosted articles. Access the articles at:  
<http://cancerdiscovery.aacrjournals.org/content/4/5/554.full.html#related-urls>

**E-mail alerts** [Sign up to receive free email-alerts](#) related to this article or journal.

**Reprints and Subscriptions** To order reprints of this article or to subscribe to the journal, contact the AACR Publications Department at [pubs@aacr.org](mailto:pubs@aacr.org).

**Permissions** To request permission to re-use all or part of this article, contact the AACR Publications Department at [permissions@aacr.org](mailto:permissions@aacr.org).

## RESEARCH BRIEF

# A Diverse Array of Cancer-Associated *MTOR* Mutations Are Hyperactivating and Can Predict Rapamycin Sensitivity

Brian C. Grabiner<sup>1,2,3,4</sup>, Valentina Nardi<sup>5</sup>, Kivanc Birsoy<sup>1,2,3,4</sup>,  
Richard Possemato<sup>1,2,3,4</sup>, Kuang Shen<sup>1,2,3,4</sup>, Sumi Sinha<sup>1</sup>,  
Alexander Jordan<sup>1</sup>, Andrew H. Beck<sup>6</sup>, and David M. Sabatini<sup>1,2,3,4</sup>

## ABSTRACT

Genes encoding components of the PI3K-AKT-mTOR signaling axis are frequently mutated in cancer, but few mutations have been characterized in *MTOR*, the gene encoding the mTOR kinase. Using publicly available tumor genome sequencing data, we generated a comprehensive catalog of mTOR pathway mutations in cancer, identifying 33 *MTOR* mutations that confer pathway hyperactivation. The mutations cluster in six distinct regions in the C-terminal half of mTOR and occur in multiple cancer types, with one cluster particularly prominent in kidney cancer. The activating mutations do not affect mTOR complex assembly, but a subset reduces binding to the mTOR inhibitor DEPTOR. mTOR complex 1 (mTORC1) signaling in cells expressing various activating mutations remains sensitive to pharmacologic mTOR inhibition, but is partially resistant to nutrient deprivation. Finally, cancer cell lines with hyperactivating *MTOR* mutations display heightened sensitivity to rapamycin both in culture and *in vivo* xenografts, suggesting that such mutations confer mTOR pathway dependency.

**SIGNIFICANCE:** We report that a diverse set of cancer-associated *MTOR* mutations confer increased mTORC1/2 pathway activity and that cells harboring these mutations are highly sensitive to rapamycin in culture and *in vivo*. These findings are clinically relevant as the *MTOR* mutations characterized herein may serve as biomarkers for predicting tumor responses to mTOR inhibitors. *Cancer Discov*; 4(5): 554-63. ©2014 AACR.

See related commentary by Rejto and Abraham, p. 513.

## INTRODUCTION

In mammals, the PI3K-AKT-mTOR pathway regulates cell size, mRNA translation, autophagy, and many metabolic processes, including lipid synthesis (1). A variety of upstream regulators control the activity of the serine/threonine

protein kinase mTOR, and many of these are deregulated in cancer, resulting in pathway hyperactivation. Such activation occurs most commonly through loss-of-function mutations in tumor suppressors, such as *PTEN*, tuberous sclerosis 1/2 (*TSC1/2*), neurofibromin 1/2 (*NF1/2*), or oncogenic mutations in *KRAS*, *PIK3CA*, or *AKT* (2). However, few cancer-associated

**Authors' Affiliations:** <sup>1</sup>Whitehead Institute for Biomedical Research; <sup>2</sup>Howard Hughes Medical Institute and Department of Biology, MIT; <sup>3</sup>Broad Institute of Harvard and MIT; <sup>4</sup>The David H. Koch Institute for Integrative Cancer Research at MIT, Cambridge; <sup>5</sup>Department of Pathology, Massachusetts General Hospital Cancer Center; and <sup>6</sup>Department of Pathology, Beth Israel Deaconess Medical Center, Harvard Medical School, Boston, Massachusetts

**Note:** Supplementary data for this article are available at Cancer Discovery Online (<http://cancerdiscovery.aacrjournals.org/>).

**Corresponding Author:** David M. Sabatini, Whitehead Institute for Biomedical Research, Nine Cambridge Center, Cambridge, MA 02142. Phone: 617-258-6407; Fax: 617-452-3566; E-mail: [sabatini@wi.mit.edu](mailto:sabatini@wi.mit.edu)

doi: 10.1158/2159-8290.CD-13-0929

©2014 American Association for Cancer Research.

mutations have been functionally characterized in *MTOR* itself, with only two reports thus far describing such mutations. In the first report (3), the authors tested six cancer-associated *MTOR* mutations and observed that two (S2215Y from a colorectal sample and R2505P from a kidney sample) conferred mTOR complex 1 (mTORC1) activation. In the second report (4), the authors identified an mTORC1-activating *MTOR* mutation (L2431P) that was present in a portion but not the entirety of a primary kidney tumor. Although these initial reports establish that activating *MTOR* mutations do arise in cancer, they were based on limited sample sets that do not reflect the diverse subtypes of cancer. More recently, cancer genome sequencing projects, such as The Cancer Genome Atlas (TCGA) and the Cancer Cell Line Encyclopedia (CCLE), have identified a vast number of somatic mutations in thousands of tumors from more than 40 cancer subtypes (5–7).

Using publicly available databases of cancer genome sequence data, we cataloged all mutations in mTOR pathway components. We annotated more than 400 samples with missense mutations in the *MTOR* gene from dozens of cancer subtypes, most of which lie within six clusters in the part of the gene that encodes the C-terminal portion of mTOR. Furthermore, through functional analyses, we identify 33 novel mTOR pathway-activating mutations, some of which affect the capacity of mTOR to interact with its partner proteins. None of the activating mutations affect the sensitivity of mTORC1 activity in cells to mTOR inhibitors, but a subset confers mTORC1 signaling resistance to nutrient deprivation. Importantly, cancer cells that naturally express a subset of the mutations are hypersensitive to the mTOR inhibitor rapamycin. These findings may have translational relevance, as rapamycin analogs (rapalogs) are clinically approved for the treatment of cancer, and several ATP-competitive mTOR kinase inhibitors are in development (8). As tumor biopsies are increasingly subjected to whole-exome sequencing, the hyperactivating *MTOR* mutations we characterize may serve as biomarkers in predicting cancer response to mTOR-targeting drugs.

## RESULTS

### Catalog of Recurring Mutations in Genes Encoding mTOR Pathway Components

To generate a comprehensive catalog of all cancer-associated missense mutations in canonical genes of the mTOR pathway, we analyzed partial genome sequencing data from the TCGA, CCLE, International Cancer Genome Consortium (ICGC), and Catalogue of Somatic Mutations in Cancer (COSMIC) databases (5–7, 9, 10). This analysis revealed that almost every gene in the mTOR pathway harbored somatic point mutations (Supplementary Table S1). To enrich for mutations that are more likely to affect pathway function, only mutations that alter the same codon more than once were counted. When normalized for gene length, this analysis revealed that *MTOR* contained the highest percentage of recurring mutations, and thus we focused most of our attention on these mutations (Supplementary Fig. S1). Collectively, through data mining and a literature search, we curated more than 400 samples with nonsynonymous *MTOR*

point mutations (Fig. 1B; Supplementary Table S2; refs. 11–17). Although the majority of these mutations are represented by only one sample in our database, approximately 40% are recurrent, most of which have not been previously described. In addition, the mutations cluster in six distinct regions of mTOR centered on highly recurrent mutations that alter amino acids C1483, E1799, T1977, S2215, L2427, and R2505 (Fig. 1C). The presence of these clusters suggests that there is a selective advantage to acquiring mutations in certain regions of the mTOR protein. Furthermore, these mutations are present in multiple cancer subtypes, with the highest number in colorectal, endometrial, and lung cancers, although these cancer subtypes are also considered to have the highest mutation rates (Fig. 1D and E; ref. 18). Interestingly, a random mutagenesis screen in the *Schizosaccharomyces pombe* mTOR homolog (*tor2*) identified activating mutations in homologous amino acid positions to many of those we find in *MTOR* to be recurrently mutated in cancer (Supplementary Table S3; ref. 19).

### mTORC1/2-Activating Mutations in *MTOR*

The prevalence of the recurrent mutations, their clustering, and correlation with activating *tor2* mutations strongly suggested that the *MTOR* mutations affect mTOR pathway activity. To test this possibility, wild-type (WT) or 10 different mTOR mutants (L1460P, C1483F, E1799K, F1888L, T1977R, V2006I, S2215Y, I2500F, R2505P, and D2512H) were expressed in cells, and phosphorylation of the mTORC1/2 substrates S6K1, 4EBP1, or AKT1 was examined (Fig. 2A–C). All the mTOR mutants conferred varying degrees of pathway activation, and, interestingly, a few displayed some substrate preference (L1460P, C1483F, S2215Y, and R2505P toward S6K1/4EBP1 and V2006I toward AKT1), implying that these mutations have greater effects on mTORC1 or mTORC2. Thus, although three pathway-activating *MTOR* mutations have previously been identified (3, 4), our initial analyses uncovered an additional eight recurrent *MTOR* mutations that activate mTORC1 and/or mTORC2.

It is well established that two activating mutations (E545K and H1047R) within the phosphoinositide 3-kinase, catalytic subunit  $\alpha$  (PI3K-p110 $\alpha$ ), encoded by the *PIK3CA* gene, can lead to mTOR pathway activation (20). To determine the degree of mTOR pathway activation conferred by mTOR mutation, S6K1 phosphorylation from cells expressing WT or S2215Y mTOR was compared with cells expressing WT or mutant PI3K-p110 $\alpha$  (Supplementary Fig. S2A and S2B). This experiment revealed that although expression of only mutant mTOR conferred mTORC1 activation, expression of either WT or mutant PI3K-p110 $\alpha$  induced mTORC1 activity.

### Nonrecurrent *MTOR* Mutations That Activate mTORC1 Signaling

We next examined in more detail the nature of the activating *MTOR* mutations, and observed that although some codons are mutated to only one other residue (e.g., E1799K), others are mutated to several different amino acids (e.g., S2215F/P/T/Y). This is reminiscent of the diverse amino acids to which the G12 residue of *KRAS* is mutated in cancers (21). We expressed 20 such *MTOR* mutations and found that many (C1483R/W/Y, F1888I, T1977K, S2215F/P, and

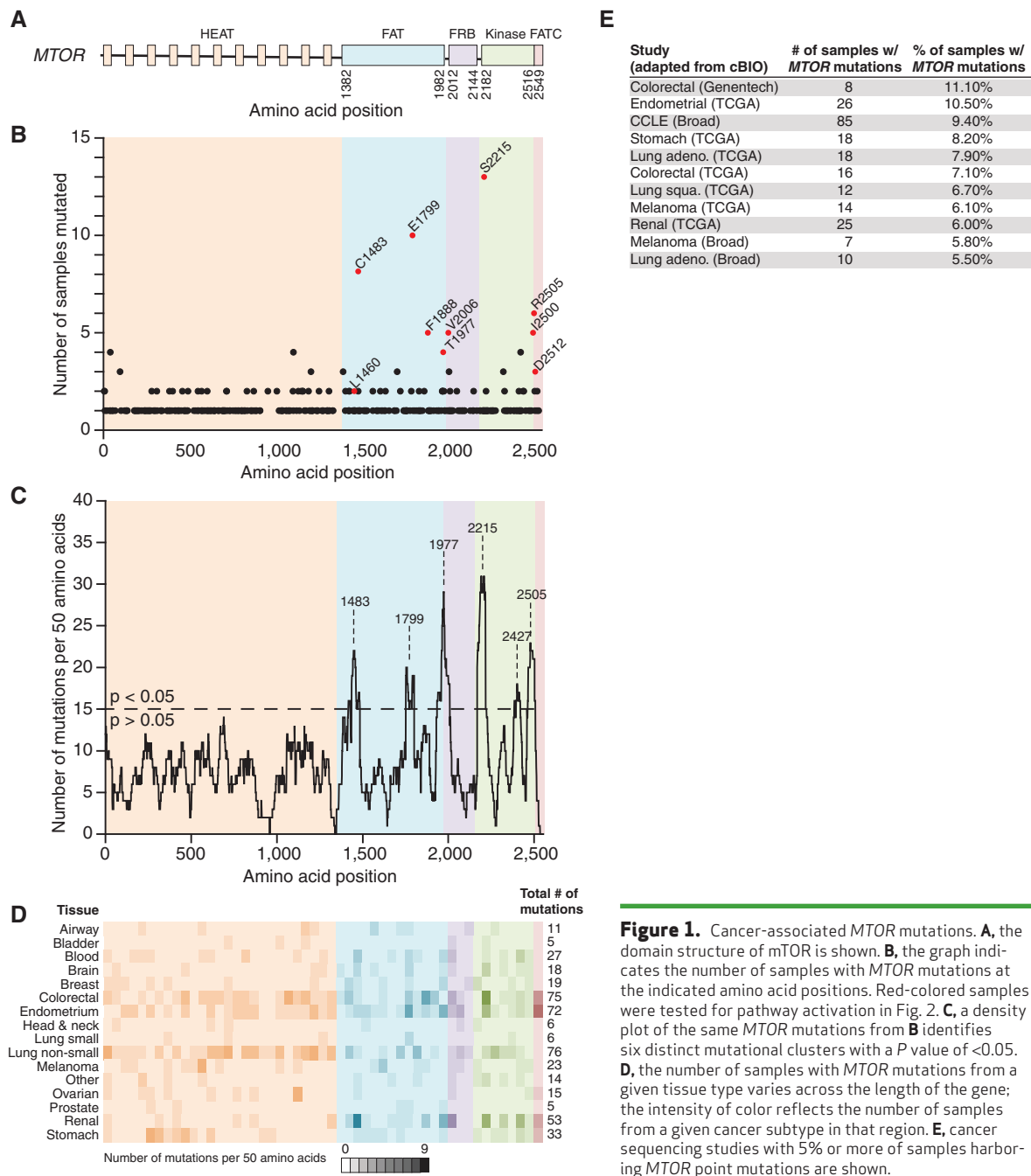
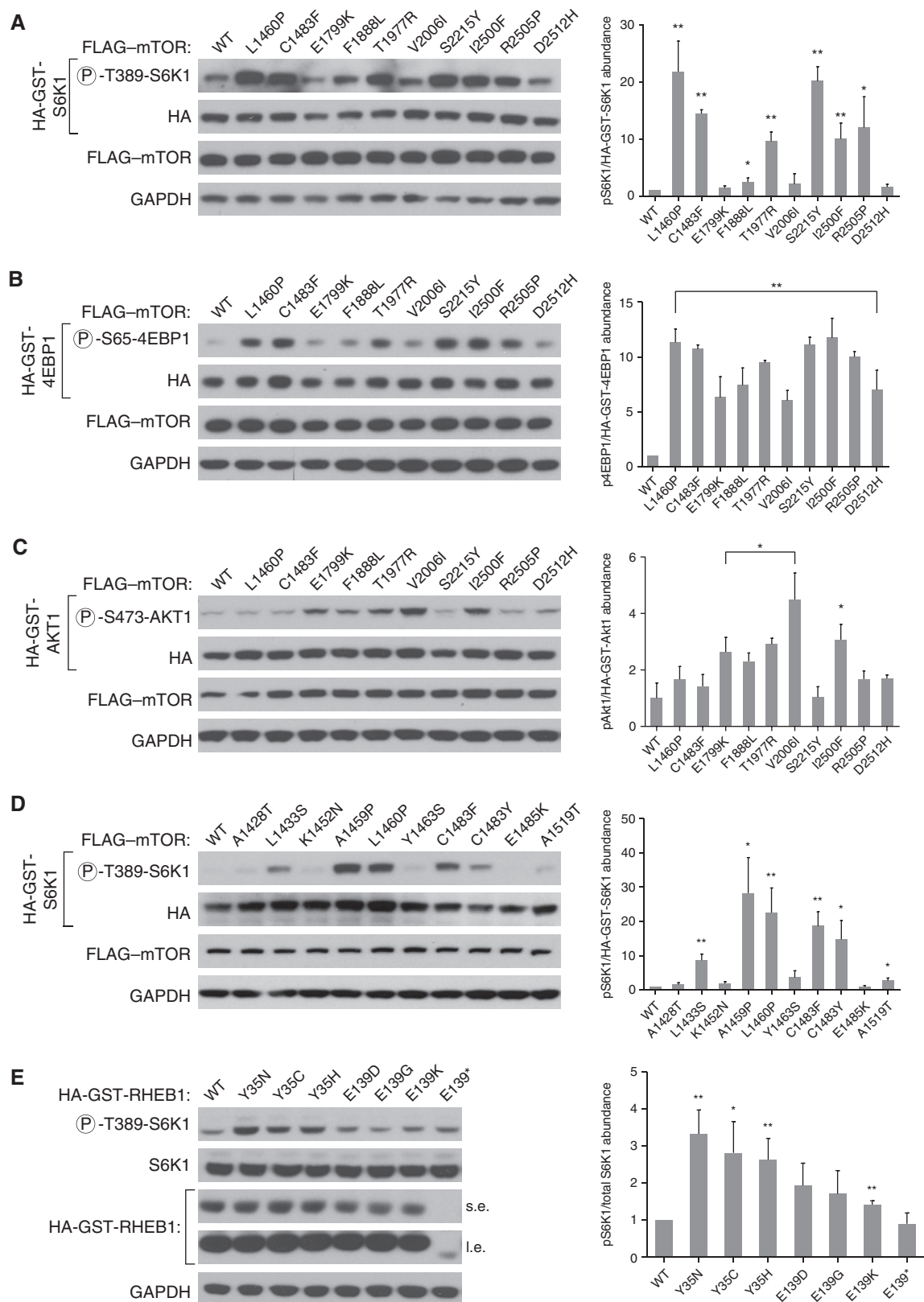


**Figure 1.** Cancer-associated *MTOR* mutations. **A**, the domain structure of mTOR is shown. **B**, the graph indicates the number of samples with *MTOR* mutations at the indicated amino acid positions. Red-colored samples were tested for pathway activation in Fig. 2. **C**, a density plot of the same *MTOR* mutations from **B** identifies six distinct mutational clusters with a *P* value of <0.05. **D**, the number of samples with *MTOR* mutations from a given tissue type varies across the length of the gene; the intensity of color reflects the number of samples from a given cancer subtype in that region. **E**, cancer sequencing studies with 5% or more of samples harboring *MTOR* point mutations are shown.

I2500M), but not all (A41P/S/T, F1888V, T1977S, V2006L, S2215T, R2505Q/\*, and D2512G/Y), led to increased S6K1 phosphorylation (Supplementary Figs. S3 and S5 and data not shown). That most of these activating mutations are found only once in our dataset implies that other nonrecurrent mutations may also activate mTORC1 signaling. To identify other such mutations, we turned our attention to the mutational clusters identified in Fig. 1 and observed that although most are represented by several tissue types, those in the C1483 cluster are particularly prevalent in kidney cancer (Fig. 1E and Supplementary Fig. S3D). Interestingly, two recent cancer genome sequencing efforts reported that kidney cancers have an increased percentage of mutations

in mTOR pathway genes, but the functional consequences of these mutations were not evaluated (13, 22). Expression of the 10 kidney cancer-associated *MTOR* mutations from the C1483 cluster revealed that in addition to the previously evaluated L1460P and C1483F/Y mutants (Fig. 1B and Supplementary Fig. S2), three nonrecurrent mutants (L1433S, A1459P, and E1519T) also induced mTORC1 pathway activity (Fig. 2D). Similarly, expression of eight nonrecurrent mutations from the S2215 cluster (N2206S, L2209V, A2210P, L2216P, R2217W, L2220F, Q2223K, and A2226S) activated mTORC1 signaling as measured by S6K1 phosphorylation, with the L2209V mutant conferring higher activation than even S2215Y (Supplementary Fig. S3E). Finally, other than



the S2215Y and R2505P mutations, the only other cancer-associated *MTOR* mutation previously characterized is L2431P from a patient with kidney cancer (4). Expression of mTOR containing this nonrecurrent mutation caused mTORC1 activation that was much weaker than that caused by expression of the S2215Y mutant (Supplementary Fig. S3F). Collectively, these results suggest that although most nonrecurrent *MTOR* mutations found in cancer are part of the mutational “noise,” there exists a diverse set of *MTOR* mutations that can drive mTORC1 pathway activity. Likely, as more cancer genomes are sequenced, the activating nonrecurrent mutations we identified will prove to be recurrent.

### Recurrent Mutations in *RHEB* Activate mTORC1

We also observed that other mTOR pathway genes, such as *RPTOR*, *RICTOR*, and *RHEB*, harbored recurrent mutations (Supplementary Table S1). Expression of *RHEB* Y35N/C/H and, to a lesser degree, E139K increased phosphorylation of endogenous S6K1 more than that of WT *RHEB* (Fig. 2E), whereas recurrent mutations in *RPTOR* (R788C) or *RICTOR* (S1101L) failed to induce any mTORC1 or mTORC2 activity (data not shown). In support of the relevance of these mutations to cancer, *RHEB* was recently highlighted as a novel cancer gene due to the presence of the Y35N mutation (23). Thus, cancer-associated mutations in either *MTOR* or *RHEB* can induce mTORC1 activity; whether this is true of other mTOR pathway genes remains to be determined.

### mTORC1/2-Activating mTOR Mutants Bind Less DEPTOR

One potential mechanism through which the mutations in *MTOR* (Fig. 2) might increase S6K1/AKT1 phosphorylation is by altering mTORC1 or mTORC2 assembly. Alternatively, or in addition, the *MTOR* mutations may diminish the binding of mTOR to its endogenous inhibitor DEPTOR, which binds to the FAT domain of mTOR (24). To test these possibilities, the interactions of exogenously expressed WT or mutant mTORs with endogenous RAPTOR, RICTOR, and DEPTOR were measured. All mutant mTOR proteins bound equally well to RAPTOR and RICTOR, suggesting that the mutations do not affect formation of either mTOR complex (Fig. 3A). In contrast, DEPTOR binding to the immunoprecipitated mTOR proteins was reduced in cells expressing the mTOR mutants as compared with WT mTOR (Fig. 3A). Given that

increased mTOR pathway activity correlates with a reduction in the mTOR–DEPTOR interaction (24), it is likely that the observed decrease in DEPTOR binding reflects the increased mTOR pathway activity caused by the *MTOR* mutations. However, two mTORC1-activating mutations that are in the FAT domain of mTOR, L1460P and C1483Y, bound much less DEPTOR than the other mutants tested (Fig. 3A), suggesting that these mutations directly perturb the DEPTOR binding site on mTOR. Consistent with this, examination of the mutations from the C1483 cluster described in Fig. 2D revealed that two other highly activating mutations in the FAT domain (A1459P and C1483Y) also strongly reduced the mTOR–DEPTOR interaction (Supplementary Fig. S4A). Although these results suggest a possible mechanism of action for a subset of activating mTOR mutations, they do not preclude other mechanisms by which *MTOR* mutations may affect mTORC1 signaling, such as by increasing the activity of the mTOR kinase domain.

### *MTOR* Mutations Do Not Affect mTORC1 Sensitivity to mTOR Inhibitors but Can Affect the Pathway Response to Nutrient Deprivation

We next considered the possibility that the mTORC1-activating *MTOR* mutants have altered sensitivity to established mTOR inhibitors. Engineered mutations in the FRB domain of mTOR, which binds the FKBP12–rapamycin complex, confer marked rapamycin resistance to mTOR (25). To test whether *MTOR* mutation alters pathway inhibition by rapamycin or Torin1 (an investigational ATP-competitive mTOR inhibitor), we used HEK-293 cells with an integrated flippase recombination site (TRES cells) to stably express WT or several different mTOR mutants (A1459P, C1483Y, E1799K, F1888I, L2209V, S2215Y, L2431P, I2500F, and R2505P), as the *MTOR* cDNA is too large to be packaged and expressed via a lentiviral delivery system (Supplementary Fig. S4B). Baseline phosphorylation of endogenous S6K1 was higher in TRES cells expressing the A1459P, L2209V, S2215Y, I2500F, and R2505P mTOR mutants than in parental or WT-expressing cells (Fig. 3B and Supplementary Fig. S4C and S4D), consistent with the results obtained upon transient expression of these mutants (Fig. 2A and D and Supplementary Fig. S3D). Importantly, mTORC1 activity in none of the TRES cells was resistant to rapamycin, Torin1, MLN0128 (an mTOR ATP-competitive inhibitor), and GDC0980 (a

**Figure 2.** mTORC1- and mTORC2-activating mutations in *MTOR* and *RHEB*. **A**, several distinct mTOR mutants induce S6K1 phosphorylation. HEK-293T cells were cotransfected with HA-GST-S6K1 and mTOR WT or mutant cDNAs in expression vectors followed by whole-cell lysis 48 hours after transfection. The lysates were then immunoblotted for the indicated proteins and the phosphorylation state of S6K1. Densitometry of phosphorylated (P) S6K1 versus HA-GST-S6K1 from three separate experiments is shown on the right; the error bars represent SEM. **B**, several distinct mTOR mutants induce 4EBP1 phosphorylation. HEK-293T cells were cotransfected with HA-GST-4EBP1 and WT or mutant *MTOR* cDNAs in expression vectors followed by whole-cell lysis 48 hours after transfection. The lysates were then immunoblotted for the indicated proteins and the phosphorylation state of 4EBP1. Densitometry of p4EBP1 versus HA-GST-4EBP1 from three separate experiments is shown on the right; the error bars represent SEM. **C**, several mTOR mutants induce AKT1 phosphorylation. HEK-293E cells were cotransfected with HA-GST-AKT1 and mTOR WT or mutant cDNAs in expression vectors followed by whole-cell lysis 48 hours after transfection and an overnight 0.5% serum starvation. The lysates were then immunoblotted for the indicated proteins and the phosphorylation state of AKT1. Densitometry of pAKT1 versus HA-GST-AKT1 from three separate experiments is shown on the right; the error bars represent SEM. **D**, the C1483 cluster harbors nonrecurrent mTORC1-activating mutations from patients with kidney cancer. HEK-293T cells were cotransfected with HA-GST-S6K1 and mTOR WT or mutant cDNAs in expression vectors followed by whole-cell lysis 48 hours after transfection. The lysates were then immunoblotted as above. Densitometry of pS6K1 versus HA-GST-S6K1 from three separate experiments is shown on the right; the error bars represent SEM. **E**, *RHEB*1 mutants induce S6K1 phosphorylation. HEK-293T cells were transfected with WT or mutant *RHEB*1 cDNAs in expression vectors followed by whole-cell lysis 48 hours after transfection. The lysates were then immunoblotted as above. Densitometry of pS6K1 versus total S6K1 from three separate experiments is shown on the right; the error bars represent SEM. In all cases, \*,  $P < 0.1$  and \*\*,  $P < 0.01$ . GAPDH, glyceraldehyde-3-phosphate dehydrogenase; s.e., short exposures; l.e., long exposures.

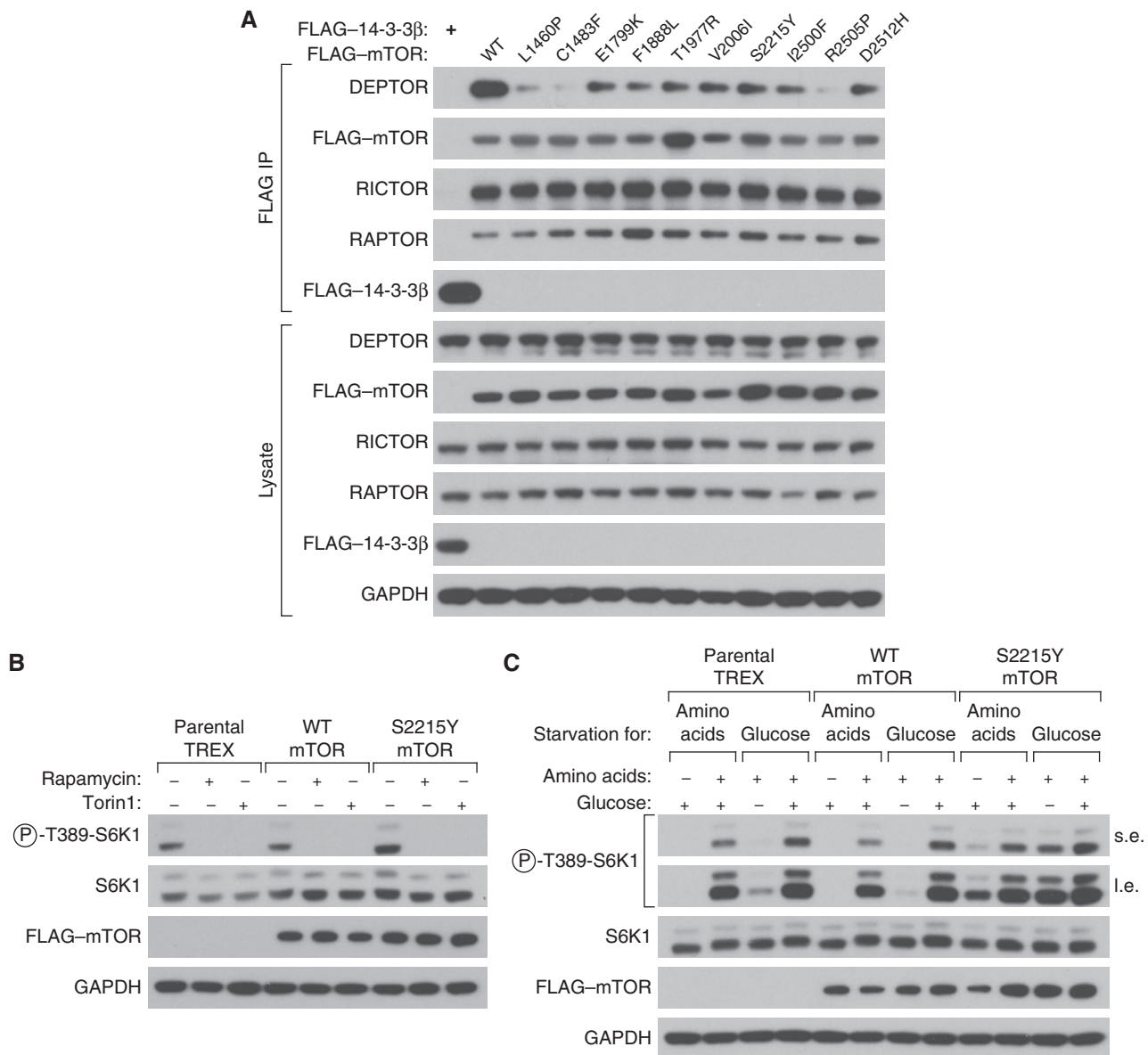


**Figure 3.** mTOR mutants bind less DEPTOR, and cells expressing the mTOR S2215Y mutation are resistant to nutrient deprivation. **A**, exogenously expressed WT and mutant mTOR coimmunoprecipitate equally well endogenous RAPTOR and RICTOR, but have reduced DEPTOR binding. HEK-293T cells were cotransfected with WT or mutant *MTOR* cDNAs in expression vectors, lysates were prepared 48 hours after transfection, and the anti-FLAG immunoprecipitates (IP) or lysates were immunoblotted for the indicated proteins. **B**, mTOR WT and S2215Y are equally sensitive to pharmacologic mTOR inhibition. Parental TREX cells or those with stable expression of mTOR WT or S2215Y were treated with rapamycin or Torin1 as described in Methods. Whole-cell lysates were then immunoblotted as in Fig. 2. **C**, the S2215Y mTOR mutant confers resistance to nutrient deprivation on S6K1 phosphorylation. Parental TREX cells or those with stable expression of mTOR WT or S2215Y were starved and re-fed amino acids or glucose as described in Methods. Whole-cell lysates were analyzed with immunoblotting as above.

dual PI3K/mTOR ATP-competitive inhibitor; Fig. 3B; Supplementary Fig. S4C and S4D). Thus, on a molecular level, although cells with *MTOR* mutations may display high levels of mTORC1/2 activity, this activity is still sensitive to pharmacologic mTOR inhibition.

The kinase activity of mTOR is tightly regulated by nutrient availability; when cells are starved of nutrients (specifically glucose and amino acids), they downregulate mTORC1 signaling, whereas retreatment of cells with these nutrients restores mTORC1-mediated signaling (26). Therefore, we

sought to determine whether any of the activating mTOR mutants affect the sensitivity of mTORC1 signaling to amino acid or glucose withdrawal. Indeed, S6K1 phosphorylation was highly resistant to deprivation of either nutrient in cells expressing several mutants (A1459P, S2215Y, I2500F, and R2505P; Fig. 3C; Supplementary Fig. S4E and S4F). This observation may be relevant in the context of developing tumors, which are often glucose starved (27, 28), where inappropriate mTORC1 activity may provide a growth advantage.

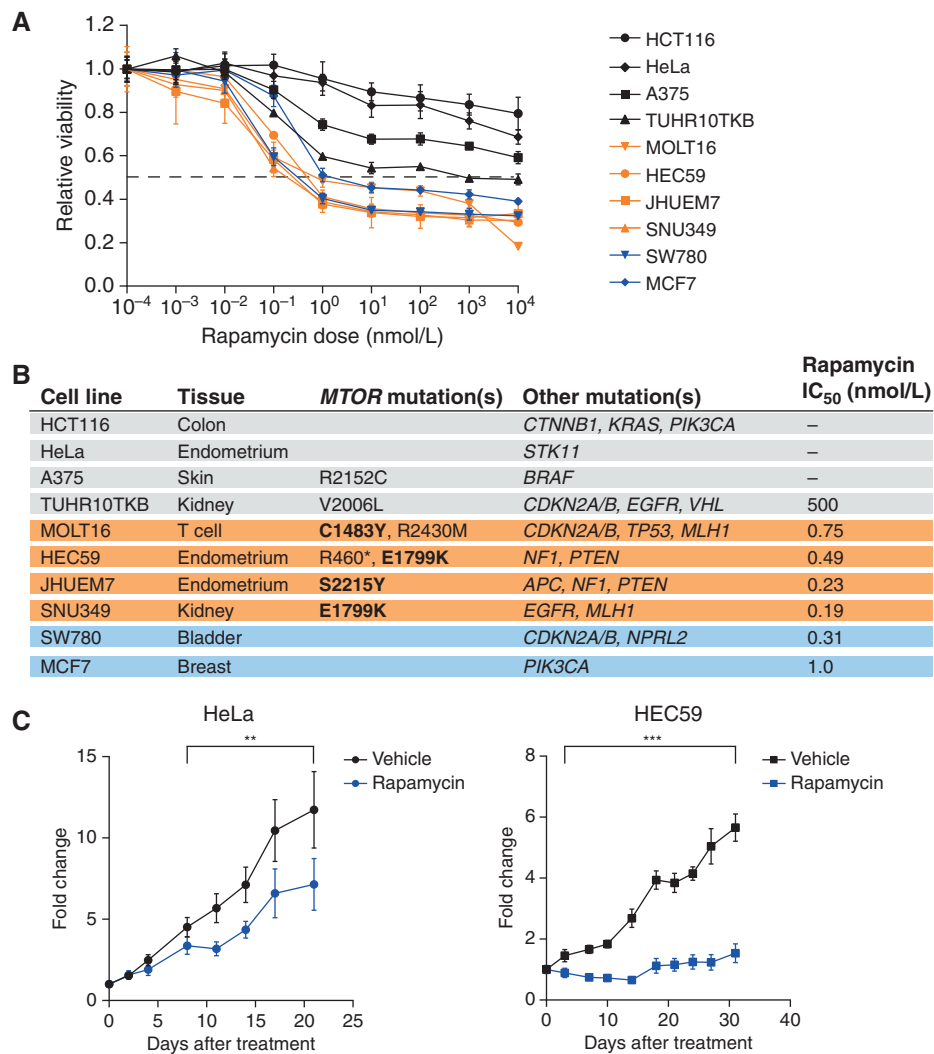


**Figure 4.** Rapamycin inhibits the proliferation of cancer cell lines with hyperactivating *MTOR* mutations. **A**, proliferation of multiple cancer cell lines with WT or mutant mTOR is differentially sensitive to rapamycin treatment. Cancer cell lines were seeded onto 96-well plates and treated with rapamycin 24 hours later, and cell viability was measured using CellTiter-Glo as described in Methods. Error bars, SD. **B**, the tissue of origin, *MTOR* mutational status, commonly mutated oncogenes/tumor suppressors, and rapamycin  $IC_{50}$  from **A** are shown for each cancer cell line. **C**, HEC59 cell xenografts are exquisitely sensitive to rapamycin treatment as compared with HeLa cell xenografts. Nine injections each of  $3 \times 10^6$  HeLa or HEC59 cells were implanted subcutaneously into the flanks of 8-week-old nude mice. One week after injection, the mice were treated daily with vehicle or rapamycin, and tumor size was measured for an additional 3 weeks. Error bars, SEM; \*\*,  $P < 0.05$ ; \*\*\*,  $P < 0.01$ .

### Cancer Cells with Hyperactivating *MTOR* Mutations Are Hypersensitive to Rapamycin *In Vitro* and *In Vivo*

To determine whether cancer cells with *MTOR* mutations are dependent on mTORC1 activity, we evaluated the impact of rapamycin on the proliferation of a set of cancer cell lines harboring WT or mutant mTOR (Fig. 4A). We identified four cell lines with mTORC1-activating *MTOR* mutations (C1483Y in MOLT16, E1799K in HEC59 and SNU349, and S2215Y in JHUEM7) and two with *MTOR* mutations that have no apparent impact on mTORC1 signaling (V2006L in TUHR10TKB and R2152C in A375; Supplementary Fig. S5A and S5B). HeLa cells were used as a negative control cell line, as they are mildly rapamycin sensitive and are WT for mTOR (7, 29). MCF7 and SW780 cells, which are also

WT for mTOR, served as positive controls for rapamycin sensitivity because the MCF7 cells harbor an activating PI3K-p110 $\alpha$  mutation (E545K), whereas the SW780 cells lack *NPRL2*, which encodes a component of the GATOR1-negative regulator of the amino acid-sensing pathway (30, 31). Importantly, only the cell lines with activating *MTOR* mutations, the PI3K-p110 $\alpha$  mutant, or the *NPRL2*-null SW780 cells were hypersensitive to rapamycin treatment (Fig. 4B). Consistent with these and published results, the growth of HeLa xenografts was partially rapamycin sensitive, whereas rapamycin completely halted the growth of HEC59 xenografts, which carry the hyperactivating mTOR E1799K mutation (Fig. 4C; refs. 32, 33). These results suggest that the presence of hyperactivating *MTOR* mutations in cancer cells may serve as biomarkers to identify tumors that are likely to respond to mTOR inhibitors.

## DISCUSSION

Early cancer genome sequencing projects led to the identification of three mutations in *MTOR* that were shown to activate mTORC1 signaling (3, 4). Here, we have identified an additional 33 previously unknown activating *MTOR* mutations (some are recurrent, others are not; Supplementary Table S4). Mechanistically, we find that the activating mutations diminish the mTOR–DEPTOR interaction and, interestingly, when mapped onto the recently solved crystal structure of mTOR, the mutations cluster in several distinct locations within the protein itself, suggesting that other activating mechanisms may exist (Supplementary Fig. S6; ref. 34). Although the mutations do not prevent pharmacologic mTOR inhibition, a subset protects against the effects of nutrient deprivation on mTORC1 signaling. Finally, we demonstrate that cell lines with activating *MTOR* mutations are particularly sensitive to rapamycin in cell culture and in xenografts, likely due to mTOR pathway dependency.

The diversity of activating *MTOR* mutations we characterized is reminiscent of the various activating mutations in the prototypical lipid kinase *PIK3CA*, which encodes for the PI3K catalytic subunit p110 $\alpha$  (35). However, unlike the activating *PIK3CA* mutations, which confer equal activation of PI3K-mediated signaling pathways, the diverse *MTOR* mutations can differentially activate mTORC1 or mTORC2, leading to either S6K1/4EBP1 or AKT1 phosphorylation, respectively. This finding is particularly relevant in a clinical setting, as patients with mTORC1-activating mutations may respond well to U.S. Food and Drug Administration (FDA)-approved rapalogs, whereas patients with mTORC2-activating mutations might best be treated with ATP-competitive mTOR inhibitors, although such inhibitors are still in clinical trials. This distinction is especially relevant for patients with mTORC2-activating mutations, because rapalogs can in some cases upregulate mTORC2 signaling through modulation of an mTORC1-dependent feedback loop (36).

Rapalog-based therapies are currently approved or are in clinical trials for several cancer subtypes, and some patients have had dramatic and durable responses to these therapies (37). Given that some cells with activating *MTOR* mutations are particularly rapamycin sensitive (Fig. 4), it is possible that some of the rapalog-responsive patients had tumors with similar mutations. Indeed, it was recently found that the tumor of a patient with bladder cancer with two activating *MTOR* mutations displayed exquisite sensitivity to rapalog-based therapy (38). Many more cancer-associated *MTOR* mutations will likely be identified in future studies, but functional evaluation of these mutations will be required to determine their impact on the mTOR pathway. As tumor sequencing becomes more common, functional studies such as ours may aid in arriving at a more personalized treatment regimen that eventually promotes patient survival.

## METHODS

### Data Acquisition and Cluster Analysis

All mutations in genes of the mTOR pathway were acquired from the cBIO, COSMIC, and ICGC databases or through a literature search with a data-freeze date of September 1, 2013. To identify

regions of mTOR significantly enriched for somatic point mutations, we determined the probability of seeing at least the observed number of mutations in a 50-amino acid sliding window with the null hypothesis being that all 463 *MTOR* mutations randomly occurring across the 2,549 amino acid protein. Specifically, we calculated a threshold for significance of at least 15 mutations per 50 amino acids by the formula

$$p = \sum_{n=k}^{463} \binom{463}{k} \times \left(1 - \frac{50}{2,549}\right)^{463-k} \times \left(\frac{50}{2,549}\right)^k$$

which equals 0.043 for  $k =$  at least 15 mutations per 50 amino acids.

### Materials

Reagents were obtained from the following sources: antibodies to hemagglutinin (clone C29F4), S6K1 (clone 49D7), phospho-T389-S6K1 (clone 108D2), and phospho-S473-AKT1 (clone D9E) from Cell Signaling Technology; antibody to glyceraldehyde-3-phosphate dehydrogenase (GAPDH; clone GT239) from Genetex; antibodies to DEPTOR and RAPTOR, X-ray film, and polyvinylidene difluoride (PVDF) membrane from Millipore; antibody to RICTOR from Bethyl; antibody to the FLAG epitope (clone M2), FLAG M2-coupled agarose beads, glucose and amino acid mixtures from Sigma; horseradish peroxidase-labeled anti-mouse and anti-rabbit secondary antibodies from Santa Cruz Biotechnology; FuGENE HD and CellTiter-Glo from Promega; X-tremeGENE 9 and Complete Protease Mixture from Roche Applied Science; QuikChange II XL from Stratagene; enhanced chemiluminescence reagent and glutathione-coupled agarose beads from Thermo; 8-week-old nude mice from Taconic; rapamycin from LC Laboratories; and MLN0128 and GDC0980 from Selleckchem. Torin1 was synthesized in the Gray laboratory (39). cDNAs for mTOR and PI3K-p110 $\alpha$  were from Addgene; expression vectors for HA-GST-S6K1, HA-GST-Akt1, and HA-GST-RHEB1 were described previously (24, 40, 41); and Flag-14-3-3 $\beta$  was a generous gift from the Yaffe laboratory. The primers used to generate the mTOR and Rheb1 mutations were from Integrated DNA Technologies and are listed in Supplementary Table S5. The HEK-293T-TREX cell system, 4% to 12% Bis-Tris SDS-PAGE gels, and 20 $\times$  MOPS buffers were from Invitrogen.

### Tissue Culture and Cell Lines

MCF7, HeLa, HEK-293T, HCT116, A375, and SW780 cells were from the American Type Culture Collection (ATCC); JHUEM7, MOLT16, NCIH446, SNU349, and TUHR10TKB cells were from the Broad Institute CCLE; HEK-293E cells were a generous gift from the Blenis Laboratory; and HEC59 cells were a generous gift from the Lippard Laboratory. The cell lines have not been reauthenticated, although those from the ATCC and the Broad Institute (Cambridge, MA) were used within 6 months of resuscitation. The HEK-293T, HEK-293E, HCT116, A375, HEC59, and TUHR10TKB cells were cultured in Dulbecco's Modified Eagle Medium (DMEM); JHUEM7 and MOLT16 cells were cultured in RPMI; and the SW780 cells were cultured in Iscove's Modified Dulbecco's Medium (IMDM). All media were prepared with 10% heat-inactivated FBS and 1% penicillin/streptomycin. All cell lines were maintained at 37°C, 5% CO<sub>2</sub>.

### Site-Directed Mutagenesis, Cloning, and TREX Cell Line Generation

All *MTOR* and *RHEB* point mutations were generated in the parental vectors using site-directed mutagenesis with the QuikChange II XL Kit according to the manufacturer's protocol. Primer sequences are listed in Supplementary Table S5. Point mutations were verified using Sanger sequencing as conducted by Eton Biosciences. The HA-GST-4EBP1 reporter vector was generated by synthesizing a gBlock

from IDT encoding for 4EBP1 and cloning it into the pRK5-HA-GST vector using *SalI* and *NotI* restriction digestion followed by ligation. WT and mutant *MTOR* cDNAs were subcloned directly from the pcDNA3 vector into the pcDNA5/FRT/TO vector using single-site *NotI* restriction digestion followed by ligation. Flag-mTOR-expressing TREX cells were generated according to the manufacturer's protocol.

### Cell Treatments, Lysis, and Immunoprecipitations

For S6K1 and AKT1 cotransfection assays,  $3 \times 10^5$  HEK-293T or HEK-293E cells per well were seeded into 6-well tissue culture plates and transfected 24 hours later with 2  $\mu$ g of mTOR-encoding plasmid and 1 ng of S6K1- or AKT1-encoding plasmid using X-tremeGENE 9 or FuGENE HD, followed by whole-cell lysis 48 hours after transfection in NP-40 lysis buffer (50 mmol/L Tris-HCl at pH 7.5, 150 mmol/L NaCl, 1% NP-40 substitute, 1 mmol/L EDTA at pH 8.0, 50 mmol/L NaF, 10 mmol/L Na-pyrophosphate, 15 mmol/L  $\text{Na}_3\text{VO}_4$ , 100 mmol/L  $\beta$ -glycerophosphate, and 1 tablet of protease inhibitor per 50 mL of buffer). Whole-cell lysates (200 to 400  $\mu$ g) were mixed with 5 $\times$  SDS sample buffer to a final concentration of 1 to 2  $\mu$ g/ $\mu$ L, boiled for 5 minutes, and then used directly for immunoblotting or frozen at  $-20^\circ\text{C}$ . For glutathione pull-down assays,  $2 \times 10^6$  HEK-293T cells were seeded onto 10-cm tissue culture plates, transfected 24 hours later with 10  $\mu$ g of mTOR-encoding plasmid and 2 ng of S6K1-encoding plasmid using X-tremeGENE 9, and lysed 48 to 72 hours after transfection in NP-40 lysis buffer. The resultant whole-cell lysates (2 to 3 mg) were incubated with 30  $\mu$ L of prewashed glutathione-coupled agarose beads in a 1-mL volume, which were rotated at  $4^\circ\text{C}$  for 2 hours, spun at 2,500 relative centrifugal force for 1 minute, and washed in 500  $\mu$ L lysis buffer three times, and the beads directly boiled in 50  $\mu$ L of 2 $\times$  SDS sample buffer. For mTOR immunoprecipitations, the cells were treated as with the glutathione pull-down, except they were lysed/washed in CHAPS buffer (50 mmol/L HEPES at pH 7.4, 150 mmol/L NaCl, 0.4% CHAPS, 50 mmol/L NaF, 10 mmol/L Na-pyrophosphate, 100 mmol/L  $\beta$ -glycerophosphate, and 1 tablet of protease inhibitor per 50 mL of buffer) and incubated with FLAG-M2-coupled agarose beads.

### Immunoblotting

Ten to 50  $\mu$ g of whole-cell lysates, 10 to 30  $\mu$ L of glutathione pull-down samples, or 10 to 30  $\mu$ L of Flag-M2 immunoprecipitates were loaded into lanes of 4% to 12% Bis-Tris SDS-PAGE gels, run at 120 V for 2 hours in 1 $\times$  MOPS buffer, and then transferred to 0.45- $\mu$ m PVDF membrane at 60 V for 2 hours in 1 $\times$  transfer buffer (100 mmol/L CAPS, 123 mmol/L NaOH, and 10% ethanol). The membranes were then immunoblotted for the indicated proteins. All primary antibodies were diluted at 1:1,000 in 5% bovine serum albumin w/v TBS+Tween 20 (TBST), with the exception of GAPDH and FLAG antibodies, which were diluted at 1:2,000. All secondary antibodies were diluted at 1:5,000 in 5% milk w/v TBST. Densitometry was performed using ImageJ, and a Student *t* test was used to determine the statistical significance.

### Rapamycin, Torin1, MLN0128, GDC0980, and Nutrient Starvation/Restimulation Treatments

For the mTOR inhibitor experiments,  $3 \times 10^5$  TREX cells per well were seeded into 6-well plates, grown for 1 day, treated with 100 nmol/L rapamycin, 250 nmol/L Torin1, 250 nmol/L MLN0128, 250 nmol/L GDC0980, or dimethyl sulfoxide (DMSO) for 60 minutes. The cells were then lysed as above. For the nutrient-deprivation experiments,  $3 \times 10^5$  TREX cells per well were seeded into 6-well plates, grown for 1 day, rinsed briefly in 1 $\times$  amino acid- or glucose-free RPMI, incubated in 1 $\times$  amino acid- or glucose-free RPMI for 60 minutes, and then stimulated with free amino acids or glucose to the levels in complete RPMI for 15 minutes.

### In Vitro Proliferation Assays

Six replicates each of 800 to 1,200 cells were seeded into 96-well plates, treated with eight doses of rapamycin 24 hours later, and assayed for ATP content using CellTiter-Glo 96 hours following rapamycin treatment according to the manufacturer's protocol.

### In Vivo Xenograft Assays

A total of  $3 \times 10^6$  cells per injection site were implanted subcutaneously into the right and left flanks of nude mice. Once tumors were palpable in all animals ( $>50 \text{ mm}^3$  volume by caliper measurements), mice were assigned randomly into rapamycin-treated or rapamycin-untreated groups, and caliper measurements were taken every 3 to 4 days until tumor burden approached the limits set by institutional guidelines. Tumor volume was assessed according to the formula  $(0.5)(W)(W)(L)$ , and a Student *t* test was used to determine the *P* values. Rapamycin (4 mg/kg) or vehicle was delivered by daily intraperitoneal injection, 100 mL per injection. All experiments involving mice were carried out with approval from the Committee for Animal Care at MIT (Cambridge, MA) and under supervision of the Department of Comparative Medicine at MIT.

### Disclosure of Potential Conflicts of Interest

No potential conflicts of interest were disclosed.

### Authors' Contributions

**Conception and design:** B.C. Grabner, V. Nardi, D.M. Sabatini  
**Development of methodology:** B.C. Grabner, R. Possemato, D.M. Sabatini  
**Acquisition of data (provided animals, acquired and managed patients, provided facilities, etc.):** B.C. Grabner, V. Nardi, K. Birsoy, R. Possemato, S. Sinha, A. Jordan, A.H. Beck  
**Analysis and interpretation of data (e.g., statistical analysis, biostatistics, computational analysis):** B.C. Grabner, R. Possemato, K. Shen, S. Sinha, A.H. Beck  
**Writing, review, and/or revision of the manuscript:** B.C. Grabner, V. Nardi, K. Birsoy, R. Possemato, S. Sinha, A.H. Beck, D.M. Sabatini  
**Administrative, technical, or material support (i.e., reporting or organizing data, constructing databases):** B.C. Grabner, A. Jordan, D.M. Sabatini  
**Study supervision:** B.C. Grabner, D.M. Sabatini

### Acknowledgments

The authors thank N. Wagle and L. Garraway for providing whole-exome sequencing data from a renal cell carcinoma patient who harbored an *MTOR* missense mutation.

### Grant Support

This research is supported in part by a postdoctoral fellowship (#118855-PF-10-069-01-TBG) from The American Cancer Society (to B.C. Grabner), The Leukemia and Lymphoma Society and The Jane Coffin Childs Fund (to K. Birsoy), NIH K99 CA168940 (to R. Possemato), and grants from the Starr Cancer Consortium, the David H. Koch Institute for Integrative Cancer Research at MIT, The Alexander and Margaret Stewart Trust Fund, and the NIH (CA103866, CA129105, and AI07389) to D.M. Sabatini. D.M. Sabatini is an investigator of the Howard Hughes Medical Institute.

Received November 27, 2013; revised March 11, 2014; accepted March 13, 2014; published OnlineFirst March 14, 2014.

### REFERENCES

- Laplanche M, Sabatini DM. mTOR signaling in growth control and disease. *Cell* 2012;149:274-93.

2. Zoncu R, Efeyan A, Sabatini DM. mTOR: from growth signal integration to cancer, diabetes and ageing. *Nat Rev Mol Cell Biol* 2011;12:21–35.
3. Sato T, Nakashima A, Guo L, Coffman K, Tamanoi F. Single amino-acid changes that confer constitutive activation of mTOR are discovered in human cancer. *Oncogene* 2010;29:2746–52.
4. Gerlinger M, Rowan AJ, Horswell S, Larkin J, Endesfelder D, Gronroos E, et al. Intratumor heterogeneity and branched evolution revealed by multiregion sequencing. *N Engl J Med* 2012;366:883–92.
5. Cerami E, Gao J, Dogrusoz U, Gross BE, Sumer SO, Aksoy BA, et al. The cBio cancer genomics portal: an open platform for exploring multidimensional cancer genomics data. *Cancer Discov* 2012;2:401–4.
6. Gao J, Aksoy BA, Dogrusoz U, Dresdner G, Gross B, Sumer SO, et al. Integrative analysis of complex cancer genomics and clinical profiles using the cBioPortal. *Sci Signal* 2013;6:p11.
7. Barretina J, Caponigro G, Stransky N, Venkatesan K, Margolin AA, Kim S, et al. The Cancer Cell Line Encyclopedia enables predictive modelling of anticancer drug sensitivity. *Nature* 2012;483:603–7.
8. Benjamin D, Colombi M, Moroni C, Hall MN. Rapamycin passes the torch: a new generation of mTOR inhibitors. *Nat Rev Drug Discov* 2011;10:868–80.
9. Forbes SA, Bindal N, Bamford S, Cole C, Kok CY, Beare D, et al. COSMIC: mining complete cancer genomes in the Catalogue of Somatic Mutations in Cancer. *Nucleic Acids Res* 2011;39(Database issue):D945–50.
10. Hudson TJ, Anderson W, Artez A, Barker AD, Bell C, Bernabe RR, et al. International network of cancer genome projects. *Nature* 2010;464:993–8.
11. Brastianos PK, Horowitz PM, Santagata S, Jones RT, McKenna A, Getz G, et al. Genomic sequencing of meningiomas identifies oncogenic *SMO* and *AKT1* mutations. *Nat Genet* 2013;45:285–9.
12. Kasaian K, Wiseman SM, Thiessen N, Mungall KL, Corbett RD, Qian JQ, et al. Complete genomic landscape of a recurring sporadic parathyroid carcinoma. *J Pathol* 2013;230:249–60.
13. Sato Y, Yoshizato T, Shiraiishi Y, Maekawa S, Okuno Y, Kamura T, et al. Integrated molecular analysis of clear-cell renal cell carcinoma. *Nat Genet* 2013;45:860–7.
14. Lee JH, Huynh M, Silhavy JL, Kim S, Dixon-Salazar T, Heiberg A, et al. *De novo* somatic mutations in components of the PI3K-AKT3-mTOR pathway cause hemimegalencephaly. *Nat Genet* 2012;44:941–5.
15. Shull AY, Latham-Schwark A, Ramasamy P, Leskoske K, Oroian D, Birtwistle MR, et al. Novel somatic mutations to PI3K pathway genes in metastatic melanoma. *PLoS ONE* 2012;7:e43369.
16. Zhang J, Grubor V, Love CL, Banerjee A, Richards KL, Mieczkowski PA, et al. Genetic heterogeneity of diffuse large B-cell lymphoma. *Proc Natl Acad Sci U S A* 2013;110:1398–403.
17. Smith LD, Saunders CJ, Dinwiddie DL, Atherton AM, Miller NA, Soden SE, et al. Exome sequencing reveals *de novo* germline mutation of the mammalian target of rapamycin (mTOR) in a patient with megalencephaly and intractable seizures. *J Genomes Exomes* 2013;2:63–72.
18. Alexandrov LB, Nik-Zainal S, Wedge DC, Aparicio SA, Behjati S, Biankin AV, et al. Signatures of mutational processes in human cancer. *Nature* 2013;500:415–21.
19. Urano J, Sato T, Matsuo T, Otsubo Y, Yamamoto M, Tamanoi F. Point mutations in TOR confer Rheb-independent growth in fission yeast and nutrient-independent mammalian TOR signaling in mammalian cells. *Proc Natl Acad Sci U S A* 2007;104:3514–9.
20. Zhao JJ, Liu Z, Wang L, Shin E, Loda MF, Roberts TM. The oncogenic properties of mutant p110alpha and p110beta phosphatidylinositol 3-kinases in human mammary epithelial cells. *Proc Natl Acad Sci U S A* 2005;102:18443–8.
21. Schubbert S, Shannon K, Bollag G. Hyperactive Ras in developmental disorders and cancer. *Nat Rev Cancer* 2007;7:295–308.
22. Network TCGAR. Comprehensive molecular characterization of clear cell renal cell carcinoma. *Nature* 2013;499:43–9.
23. Lawrence MS, Stojanov P, Mermel CH, Robinson JT, Garraway LA, Golub TR, et al. Discovery and saturation analysis of cancer genes across 21 tumour types. *Nature* 2014;505:495–501.
24. Peterson TR, Laplante M, Thoreen CC, Sancak Y, Kang SA, Kuehl WM, et al. DEPTOR is an mTOR inhibitor frequently overexpressed in multiple myeloma cells and required for their survival. *Cell* 2009;137:873–86.
25. Dumont FJ, Staruch MJ, Grammer T, Blenis J, Kastner CA, Rupperecht KM. Dominant mutations confer resistance to the immunosuppressant, rapamycin, in variants of a T cell lymphoma. *Cell Immunol* 1995;163:70–9.
26. Efeyan A, Zoncu R, Sabatini DM. Amino acids and mTORC1: from lysosomes to disease. *Trends Mol Med* 2012;18:524–33.
27. Urasaki Y, Heath L, Xu CW. Coupling of glucose deprivation with impaired histone H2B monoubiquitination in tumors. *PLoS ONE* 2012;7:e36775.
28. Hirayama A, Kami K, Sugimoto M, Sugawara M, Toki N, Onozuka H, et al. Quantitative metabolome profiling of colon and stomach cancer microenvironment by capillary electrophoresis time-of-flight mass spectrometry. *Cancer Res* 2009;69:4918–25.
29. Gulhati P, Zaytseva YY, Valentino JD, Stevens PD, Kim JT, Sasazuki T, et al. Sorafenib enhances the therapeutic efficacy of rapamycin in colorectal cancers harboring oncogenic KRAS and PIK3CA. *Carcinogenesis* 2012;33:1782–90.
30. Bar-Peled L, Chantranupong L, Cherniack AD, Chen WW, Ottina KA, Grabiner BC, et al. A tumor suppressor complex with GAP activity for the Rag GTPases that signal amino acid sufficiency to mTORC1. *Science* 2013;340:1100–6.
31. Meric-Bernstam F, Akcakanat A, Chen H, Do KA, Sangai T, Adkins F, et al. PIK3CA/PTEN mutations and Akt activation as markers of sensitivity to allosteric mTOR inhibitors. *Clini Cancer Res* 2012;18:1777–89.
32. Shoji K, Oda K, Kashiyama T, Ikeda Y, Nakagawa S, Sone K, et al. Genotype-dependent efficacy of a dual PI3K/mTOR inhibitor, NVP-BEZ235, and an mTOR inhibitor, RAD001, in endometrial carcinomas. *PLoS ONE* 2012;7:e37431.
33. Totary-Jain H, Sanoudou D, Dautriche CN, Schneller H, Zambrana L, Marks AR. Rapamycin resistance is linked to defective regulation of Skp2. *Cancer Res* 2012;72:1836–43.
34. Yang H, Rudge DG, Koos JD, Vaidialingam B, Yang HJ, Pavletich NP. mTOR kinase structure, mechanism and regulation. *Nature* 2013;497:217–23.
35. Vogt PK, Hart JR, Gymnopoulos M, Jiang H, Kang S, Bader AG, et al. Phosphatidylinositol 3-kinase: the oncoprotein. *Curr Top Microbiol Immunol* 2010;347:79–104.
36. O'Reilly KE, Rojo F, She QB, Solit D, Mills GB, Smith D, et al. mTOR inhibition induces upstream receptor tyrosine kinase signaling and activates Akt. *Cancer Res* 2006;66:1500–8.
37. Sonpavde G, Choueiri TK. Precision medicine for metastatic renal cell carcinoma. *Urol Oncol* 2014;32:5–15.
38. Wagle N, Grabiner B, Van Allen E, Hodis E, Jacobus S, Supko J, et al. Activating mTOR mutations in a patient with an extraordinary response on a phase I trial of everolimus and pazopanib. *Cancer Discov* 2014 Mar 13. [Epub ahead of print].
39. Liu Q, Chang JW, Wang J, Kang SA, Thoreen CC, Markhard A, et al. Discovery of 1-(4-(4-propionylpiperazin-1-yl)-3-(trifluoromethyl)phenyl)-9-(quinolin-3-yl)benzimidazole as a highly potent, selective mammalian target of rapamycin (mTOR) inhibitor for the treatment of cancer. *J Med Chem* 2010;53:7146–55.
40. Burnett PE, Barrow RK, Cohen NA, Snyder SH, Sabatini DM. RAFT1 phosphorylation of the translational regulators p70 S6 kinase and 4E-BP1. *Proc Natl Acad Sci U S A* 1998;95:1432–7.
41. Sancak Y, Peterson TR, Shaul YD, Lindquist RA, Thoreen CC, Bar-Peled L, et al. The Rag GTPases bind raptor and mediate amino acid signaling to mTORC1. *Science* 2008;320:1496–501.